2017 International Nuclear Atlantic Conference - INAC 2017
Belo Horizonte, MG, Brazil, October 22-27, 2017
ASSOCIAÇÃO BRASILEIRA DE ENERGIA NUCLEAR – ABEN

Agência Brasileira do ISBN
ISBN 978-85-99141-07-6
9 788599 141076

STRUCTURAL AND MICROSTRUCTURAL ANALYSIS OF THE U-GD-O SYSTEM USING X-RAY DIFFRACTION DATA

Gaspar Darin[1], Kengo Imakuma[1], Luis G. Martinez[1], Xabier M. Turrrilas[2], Rodrigo U. Ichikawa[1], André S. B. Silva[1], Michelangelo Durazzo[1], Humberto G. Riella[1] and Elita Urano[1]

[1] Instituto de Pesquisas Energéticas e Nucleares (IPEN / CNEN - SP)
Centro de Combustíveis Nuclear
Av. Professor Lineu Prestes 2242
05508-000 São Paulo, SP
gaspardarin@gmail.com ; kimakuma@ipen.br ; lgallego@ipen.br ; ichikawa@usp.br ;
andre.santos.silva@ipen.br ; mdurazzo@ipen.br ; riella@enq.ufsc.br ; elitaucf@ipen.br

[2] Institute of Material Science of Barcelona (ICMAB)
Campus de la UAB 08193 Bellaterra
08193 Bellaterra, Barcelona, Espanha
xturrillas@icmab.es

ABSTRACT

Gadolinium is one of the best neutron absorber materials and its usage can be considered as a burnable poison for Light Water Reactors (LWR) and as a sacrificial material in Sodium Fast Reactor (SFR). Most of the experiments in the literature focus on nuclear fuel with up to 12 wt% Gd_2O_3. Recently, the phase diagram and melting point has been investigated for high contents of Gd_2O_3 in the U-Gd-O system, that means a solid solution of the composition $(U_{1-x}, Gd_x)O_2$ for $0<x<100\%$. In this work, we present the analysis of the U-Gd-O system for high contents of Gd_2O_3 using X-ray diffraction data. Rietveld analysis was applied to obtain cell parameters, atomic positions and atomic displacement factors and compared with literature avaliable. Also, the quantification of phases was performed for the different contents of Gd_2O_3 in the system. Finally, mean crystallite sizes were determined and correlated with the weight fraction of the phases.

1. INTRODUCTION

The U–Gd–O system is very useful for nuclear industry since gadolinium is a good neutron absorber material. In low contents, gadolinium is used as burnable absorbers (called too of burnable poison) in Light Water Reactors (LWR) [1]. A burnable poison is a material used in reactors to afford a negative moderator coefficient at the beginning of reactor life and help shape core power distributions [2]. For high contents (>40wt%), U-Gd-O system is used as sacrificial material in Sodium Fast Reactor (SFR) in order to increase the safety of SFR reactors. In this way, many accidents as a result of overheating could be avoided, or at least, their consequences reduced [3]. Gadolinium-doped UO_2 pellets are prepared by sintering gadolinia and urania powders. After all, the homogenization of UO_2 and Gd_2O_3 powders is hard to achieve. That is the reason why a detailed knowledge of the thermodynamic phase diagram is necessary.

The UO_2 naturally occurs in an isostructural solid, where each uranium atom is surrounded by eight oxygen atoms in a cubic arrangement called fluorite [4]. Pure gadolinia exists mostly under three different crystalline forms: hexagonal, monoclinic and cubic BCC [5]. A

rhombohedral phase is also known but only in very specific conditions [6]. The cubic form is the prevailing structure because is more thermodynamically stable at ambient temperature and atmospheric pressure. The monoclinic and rhombohedral phase can also exist simultaneously with the cubic phase at room conditions. None of them, was observed in the system and therefore won't be considered in this assessment.

U–Gd–O system has been studied commonly studied for low Gd content samples (<40 wt% of Gd_2O_3) [6]. In this circumstances, a cubic FCC phase was found [7,8] after sintering under H_2 atmosphere. The mixture forms a solid solution, where Gd^{3+} cations were arranged at U^{4+} sites in UO_2 fluorite structure. Beals et al 1969 has measured the lattice parameter after air sintering showing that these parameters got smaller due to oxidation [4]. For Gd contents larger than 0.50 gadolinium-to-metal atomic ratio (Gd/M), a BCC phase was found in co-existence of fluorite by Durazzo et al 2009 [8]. But until today exists many divergences about the arrangement for U-Gd-O mixtures with high contents of gadolinia. In this work, a structural and microstructural analysis was done for a set of samples with composition $(U_{1-x}, Gd_x)O_2$ for Gd/M values ranging from $0.60<x<0.90$, or in weight contents, between 0.50 to 0.85.

2. MATERIALS AND METHODS

2.1. Material synthesis

The $(U_{1-x}Gd_x)O_2$ solid solutions samples have been prepared by coprecipitation method. The coprecipitation method is largely used in nuclear fuel industry to provide a $(U,Gd)O_2$ homogeneity better than the obtained by mechanical blending [2]. The set of samples varies between 50 and 85 wt% Gd_2O_3, main characteristics are resumed in Table 1. The pellets were prepared by wet route in according to the method reported in detail at [8,9]. The sintering step was done on a tungsten crucible in flowing Ar H_2 5% and the heating rate of 1 °C/min. The set of samples was heated up to 1650 °C during 3 h and the cooling down rate was 1 °C/min.

Table 1: Set of samples in terms of weight Gd-to-Metal (wt%) and the molar quantity.

wt% Gd2O3	Gd/M (atomic ratio)	Gd/U (atomic ratio)
50.18	0.60	1.90
53.34	0.63	1.92
56.48	0.66	1.94
61.04	0.70	1.98
66.43	0.75	3.02
74.11	0.81	3.08
85.41	0.90	3.17

*M denotes the sum of U and Gd atoms.

2.2. Microstructural analysis: Warren-Averbach method

X-ray line profile analysis (XLPA) was developed by Scherrer [10] in 1918 found that the breadth of a diffraction line is related to the finite size of the diffraction crystal. Later, Langford [11] related the breadth with finite size of diffraction and microstrain, after these considerations, Warren and Averbach 1950 developed a very rigorous method which it does not assume any shape of the diffraction peaks for determination of crystallite size and microdeformation [12]. The Fourier Transform is applied in two at least two parallel planes of the same reflection (hkl), allowing the calculation of mean area of crystallite size, root mean square strain (RMSS), and crystallite size distribution. The detailed description is found in [12,13].

2.3. Structural analysis

The Rietveld method is a modelling procedure which a set of intensities comprising the calculated pattern, determined according to a model defined previously, is fitted by non-linear least squares to the correlative experimental pattern. Structural parameters (lattice parameters, atomic positions, site occupancies and thermal parameters), background function, scale factors for quantitative phase analysis, among others parameters can be investigated in Rietveld analysis [14]. Least squares Rietveld refinement is designed to minimize the residual summed over the n points in the pattern at which the intensity is sampled [15]. The most meaningful being the weighted profile R factor (R_{wp}) is the quantity being minimized by least squares during refinement, see Equation 1.

$$R_{wp} = \left[\frac{\sum w_i (y_{io} - y_{ic})^2}{\sum w_i y^2{}_{io}} \right]^{1/2} \quad (1)$$

where y_{io} and y_k are the observed and calculated intensity at the i^{th} step, respectively, and w_i is the weight assigned to each observation [16].

Quantitative phase analysis results are obtained when a known amount of internal standard is combined to the polyphasic compound and the whole pattern is refined using the Rietveld method. The concentration for each crystalline phase, W_k, is given by Equation 2

$$W_k = \frac{W_s (ZMV)_k \cdot S_k}{(ZMV)_s \cdot S_s} \quad (2)$$

where W_s is the known wt% of the internal standard in the mixture, S is the Rietveld scale factor, ZM is the unit-cell mass and V is the unit-cell volume.

3. RESULTS

3.1. Diffraction patterns of the powdered samples

XRD measurements were performed on powdered samples using the D8 Advance Bruker diffractometer with a copper X-ray source ($k_{\alpha 1}$ = 1.54056 Å and $k_{\alpha 2}$ = 1.5444 Å). A nickel filter was used to filter copper k_{β} wavelength. Angular step was of 0.02° and 10 seconds of count per point. Diffractograms were obtained by Bragg-Brentano geometry for Powder Diffraction Method. Crystalline phases in the XRD patterns were identified using Bruker® Diffracplus EVA v16 software to search the ICDD® Powder Diffraction File. The crystal structures of the phases were extracted from the FIZ Karlsruhe Inorganic Crystal Structure Database (ICSD 2009/2) in the form of crystallographic information files (CIF files). Bruker® (2008) TOPAS v4.2 was used to perform Rietveld quantitative analysis. The experimental data is reported in the Fig. 1.

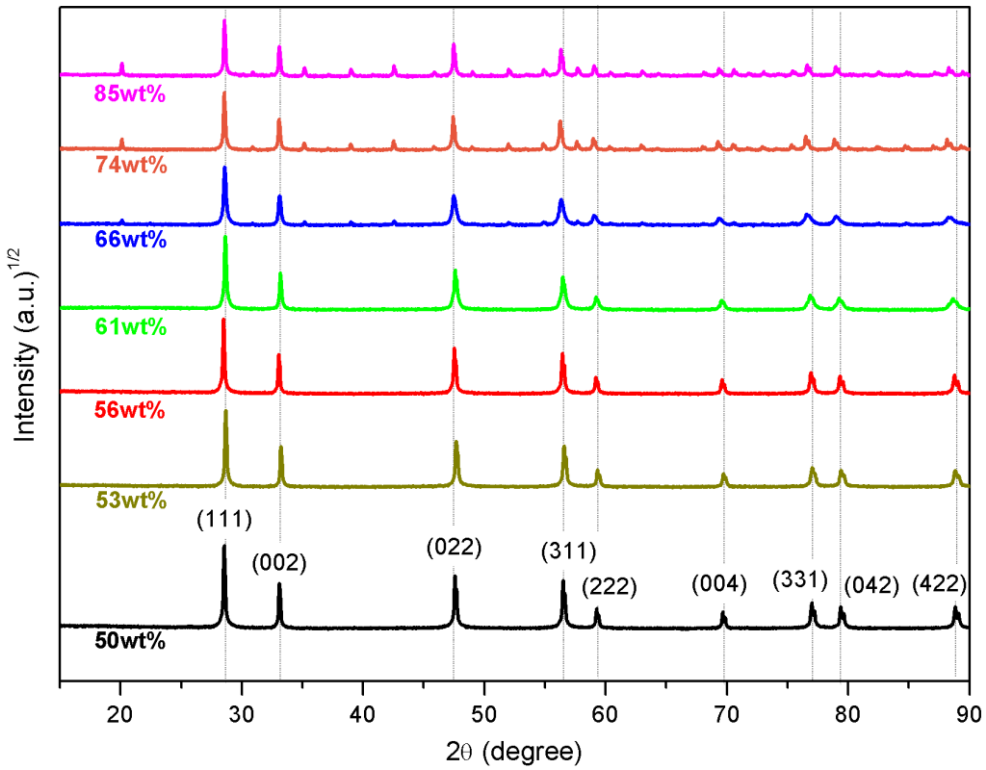

Figure 1 – Experimental XRD data for powder samples presented in Table 1. The nomenclature wt% is the quantity of gadolinia in mass of the mixture UO_2-Gd_2O_3.

3.2. Rietveld refinement results

The model of structure for Rietveld refinement was based on two cubic phases: FCC and BCC, both under the reference of pure phase at room conditions for UO_2 and Gd_2O_3. The CIF files handled were from ICSD with codes 160814 for FCC (2008) and 184595 for BCC (2012). All the results for Rietveld refinement can be seen on Table 2. The peak shape for microstructural refinement was run in according to a standard sample of Y_2O_3.

Table 2: XRD results from Rietveld refinement by TOPAS.

wt% Gd2O3	Cubic FCC Lattice parameter (Å)	Cubic BCC Lattice parameter (Å)	Cubic FCC Phase quantity	Cubic FCC LVol (nm)	Cubic BCC LVol (nm)
50.18	5.3859(1)	10.819(3)	90(1)%	216(14)	21(4)
53.34	5.3935(2)	10.835(5)	93(1)%	152(12)	26(6)
56.58	5.3867(1)	10.823(4)	91(1)%	180(9)	30(6)
61,.04	5.4060(4)	10.842(2)	90(2)%	140(18)	42(10)
66,.83	5.4249(2)	10.8543(4)	59(1)%	66(4)	129(15)
74.11	5.4302(1)	10.8601(2)	24(1)%	161(10)	293(19)
85.81	5.4223(2)	10.8433(1)	10(1)%	159(22)	254(29)

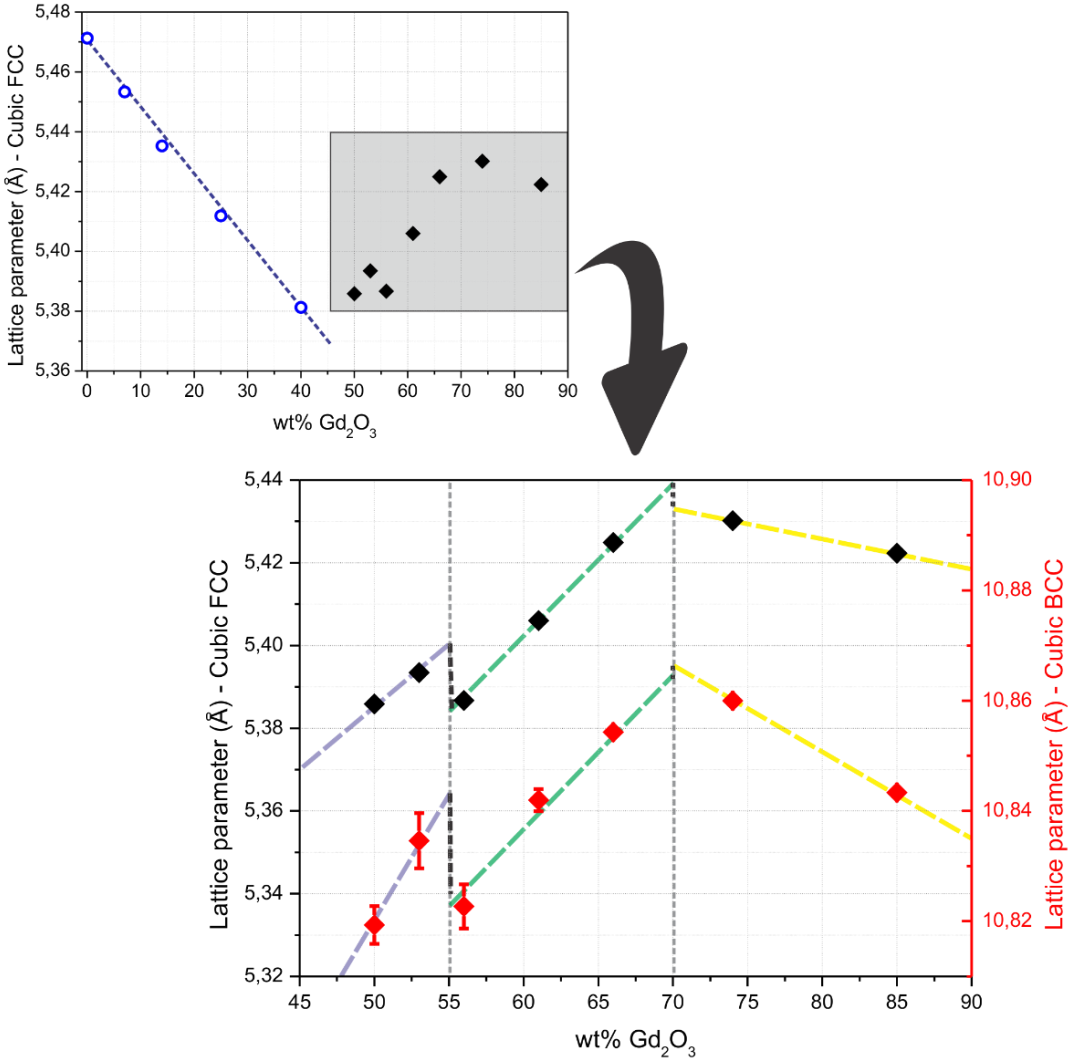

Figure 2: At the top, lattice parameters from [17] in blue, including the linear fitting, and experimental data of FCC phase in black. At the bottom, gray region in detail for both phases. Black represents the cubic FCC phase and red the cubic BCC.

The lattice parameters results are shown on Fig. 2. This study suggested a division in three regions: purple line (positive slope), green line (higher positive slope than purple) and yellow (negative slope). Baeda et al 2015 shows that the lattice parameter variation complies with the Vegard's Law until 40 wt% (0.5 mol) of gadolinium in the U-Gd-O system [17]. His results are shown on the top of Figure 2. Blue dots are the data and the blue dashed line is the linear fitting presented on Equation 3:

$$a(\text{Å}) = 5.47127(8) - 0.179(1) \cdot x \qquad (3)$$

where a is the lattice parameter of fluorite and x is the quantity of Gd contents in mol [17].

Investigations for contents higher than x>0.5 of $(U_{1-x}Gd_x)O_2$ system hasn't been done very often. The previous studies didn't present a U-Gd lattice parameter diagram with good resolution and there's no consent about how many phases exists in this region yet. The results of this work is shown in black balloons side-by-side with Baeda at the top of Fig. 2 [17]. The gray area is the region of interest. As mentioned, the Rietveld refinement was performed on two cubic phases FCC and BCC. The lattice parameters for FCC phase is still presented in black balloons, the BCC phase results is shown in red balloons, both in detail at the bottom of Fig. 2.

Quantitative Phase Analysis (or simply QPA) was adopted in this investigation for two reasons. First, the set of samples are a mixture of two pure compounds. Second, the relative intensities of peak reflections are different of a pure phase pattern. This assertion is presented in Fig.3 .

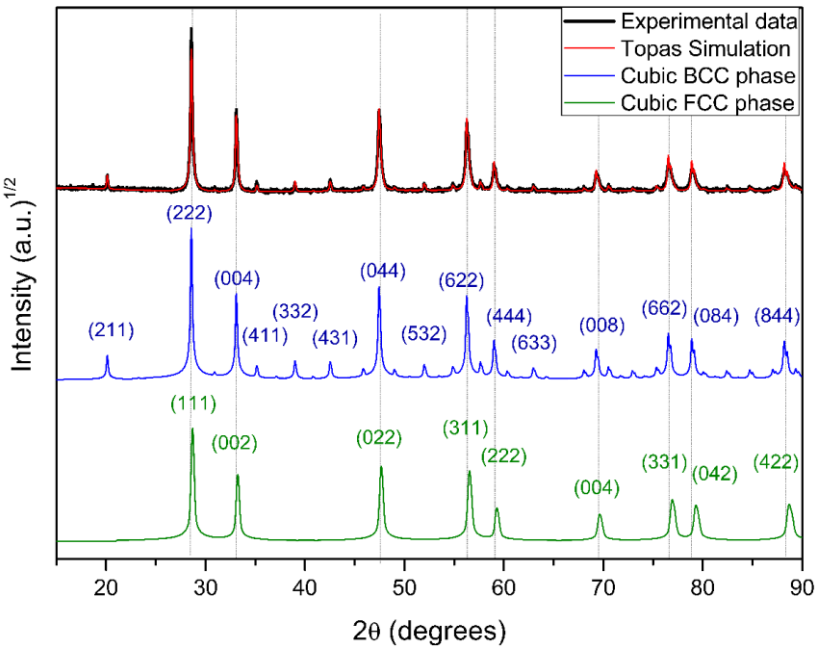

Figure 3: Experimental results for the 66 wt% sample.

Although the XRD patterns showed huge evidences of a biphasic behavior, the peak intensities were not doublets. These doublets were not observed since the unit cell of Gd_2O_3 BCC phase

is geometrically similar to the four UO_2 - FCC cubic assembled in a block. In other words, the lattice parameter of BCC phase is multiple of FCC phase. This specific condition generated a set of overlapping peaks. In the Fig. 3, is possible to see the XRD data of sample 66 wt% in comparison with FCC and BCC phases. This sample was chosen because the proportion of phases seems approximately equivalent. At top of Fig. 3, experimental data in black and Topas simulation in red. The blue graphic and the green one, are the BCC and FCC phases with hkl index, respectively. The QPA results can be seen at top of Fig. 4.

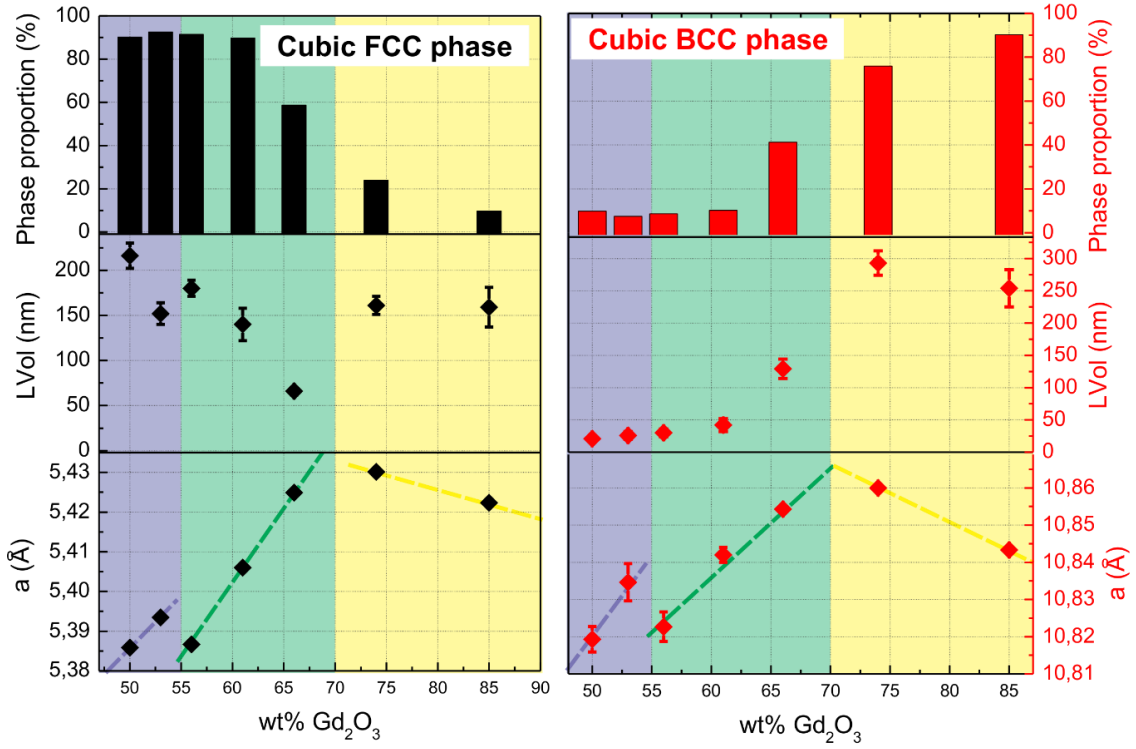

Figure 4: At the top, QPA results. Microstructural parameter LVol at the middle. Lattice parameter diagram at the bottom.

The microstructural analysis calculates a distribution of possibility of crystallite sizes [14]. The parameter estimated by Topas refinement calculates the volume weighted mean column heights. This quantity is called LVol and are shown at the middle of Figure 4. The parameter LVol is discussed in details by Balzar et al 2004 [18]. At the bottom of Fig. 4, we can find the lattice parameters results for both phases. From the tendency of results, the graphics of Figure 4 were subdivided into three regions: purple, for the first two points; green, next three concentrations; and yellow, the last two samples. More reasons for this subdivision will be discussed further.

3.3. Warren-Averbach method for microstructural analysis

The Warren-Averbach method is used for a rigorous microstructural characterization. This method only can be applied in single phase systems. That's require the disengagement of the

phases in the diffraction patterns of polyphasic systems. This dissociation can be obtained through the Rietveld refinement by Topas simulation. The broadening of peaks reveals the microstructural information, lattice strain and crystallite size distribution for example. The Warren-Averbach calculations were performed on the most intensive peak of each phase using Python routines. At the top of Fig. 5 is found the broadening peaks behavior. On the left, for cubic FCC phase and, on the right, BCC phase. At the bottom of Fig. 5 is shown the normalized crystallite size distribution.

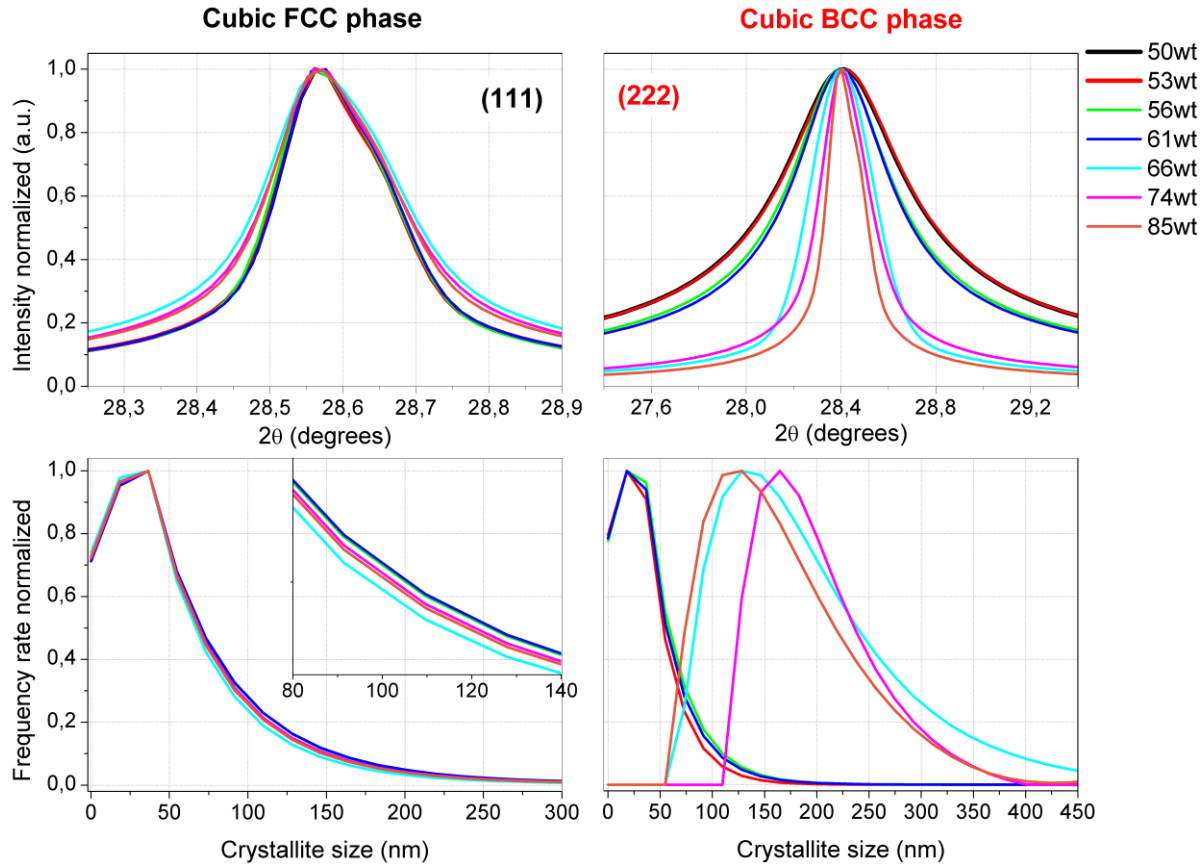

Figure 5: Microstructural graphics results. Above, he broadening of peaks (111) and (222) of FCC and BCC phases, respectively. Below, the distribution of crystallite sizes.

4. DISCUSSION

According to the second figure, the XRD patterns demonstrated strong evidences of two cubic phases. The FCC phase predominates for the samples in lower Gd_2O_3 than 66 wt% quantity, and consequently, BCC phase prevailed over this. This evidence was quantified and presented in the graphics at the top of the Fig. 5. The monoclinic phase was used in refinements too, but it didn't show significant portion according to QPA results. Consequently, the characterization models of this study are based in only two cubic phases, FCC and BCC.

The Rietveld refinement results were in graphics under proposal of the three zones, Fig. 4: 1) purple, locate between 50 and 55 wt% of Gd_2O_3; 2) green, between 55 and 70 wt%; and 3) yellow, for values superior to 70 wt%. This division was based on behavior of the data from

all parameters obtained in refinement, except LVol green region of Cubic BCC phase. The crucial circumstances chosen were the crack of lattice parameter expansion at 56 wt% and the start of lattice contraction after 74 wt%.

The yellow sector shows a contraction of lattice parameter for both phases, but BCC phase vary two times more than FCC. This contraction behavior could be expected based on the difference of ionic radius between uranium and gadolinium, r_{Gd}^{3+} = 0.1053 nm and r_{U}^{4+} = 0.1001 nm and oxidation state [19]. The total amount of Gd_2O_3 is much greater than UO_2, so it is possible the uranium atoms are inside the cubic BCC structure. The phase proportion results show the cubic BCC phase increase according to the gadolinia quantity, that is naturally understandable.

The purple zone has high signs of being composed essentially by a single phase of symmetry space group Fm-3m, FCC structure type. This assertion was established on the low values results for BCC phase in the QPA analysis. Even in very low proportion, the BCC phase expand as FCC. The expanding of lattice is related to the valence state +3 of Gd and the oxidation state of uranium [20].

Finally, the green region showed up particularly interesting. The upward trend from the purple sector is abruptly cracked at the 56 wt% Gd_2O_3 content. After that, the lattice parameter expands but in a different rate of the previous zone. The LVol parameter, at middle of Fig. 5, indicates that BCC phase contain bigger crystallites in high proportions of gadolinia. While the FCC phase kept its value almost constantly for all over the range, except for 66 wt% sample. The LVol parameter of BCC phase followed the growing trend of his lattice parameter, while for FCC phase, it occurs the opposite. The green zone demonstrates very strong evidences of biphasic system. This phase condition has been suggested by Pieck et al 2015 previously at 66 wt% which is totally in accordance with the results of this assessment [1].

The Warren-Averbach method shows that the FCC cubic structure has a constant crystallite size distribution, checked at the bottom left side of the Fig. 5. That is consent with the LVol microstructural parameter curve from Rietveld method. Differently the of FCC, the BCC structure suggest a tendency of increasing the crystallite magnitude for higher concentrations of Gd_2O_3. The results of Warren-Averbach method are perfectly consistent with the LVol parameter. The first four concentrations have smaller crystallite sizes and similar values. The concentrations 61, 66 and 74 wt% behave such a linear raise. And the last sample, 85 wt% of gadolinia, demonstrates a contraction of crystallite size. That could be the effect of a rearrangement of the crystalline structure. The order of magnitude of crystallite size by Warren-Averbach is compatible with Rietveld method, that was found between 30 and 300 nm. A divergence of around 50 nm was expected because the difference of methodologies [18]. Values very close of this variation was observed for the BCC phase results. The FCC phase differed more, resulting in smaller values for the Warren-Averbach method.

The strain for both methods was practically zero. Which is in accordance with the characteristics of ceramic materials and the high temperature treatment submitted.

5. CONCLUSION

1. A multiphasic zone was observed mainly in the green region. This study characterized the results based only in two phases. Consequently, the Rietveld refinement of these concentrations could be more accurate, in other words, lower R_{wp} parameter. Which may be the presence of other less intense phase. More investigations are necessary in this range of U-Gd-O system.
2. Although this investigation has worked with a set of seven samples, the several non-expected behaviors of the structure requires a larger number of U-Gd-O mixtures to generate more consistent results.
3. Microstructural analysis results were compatible with a very regular crystallite size distribution of FCC phase for all over the range. While BCC phase showed an increase at the green zone and decrease at the yellow region of crystallite size most probable value.
4. The crystallite size found was between 30 and 300 nm.

ACKNOWLEDGMENTS

The first autor would like to thank the Nuclear Fuel Center (CCN) of Energetic and Nuclear Research Institute initiative for sponsoring these studies, Dr. Riella and Dr. Imakuma for her assistance and guidance on this project, Dr. Durazzo for his assistance in developing the set of samples and MSc. André Silva for his essential cooperation in this work.

REFERENCES

1. D. Pieck, L. Desgranges, P. Matheron, H. Palancher, “Evidence of a new crystalline phase in U-Gd-O phase diagram,” *Journal of Nuclear Materials*, **Volume 461**, pp.186-192 (2015).
2. H. G. Riella, M. Durazzo, M. Hirata, R. A. Nogueira, “UO_2-Gd_2O_3 solid solution formation from wet and dry processes” *Journal of Nuclear Materials*, **Volume 178**, pp.204-2011 (1991).
3. C. Journeau, P. Fourquart, R. Domenger, P. Allegri, “Hypoeutectic melting in the UO_{2-x}-Gd_2O_3 system” *Journal of Nuclear Materials*, **Volume 488**, pp.287-294 (2017).
4. R.J. Beals, J.H. Handwerk, B.J. Wrona, “Behavior of Urania-Rare-Earth Oxides at High Temperatures” *J. Am. Ceram. Soc*., **Volume 52**, pp. 578 (1969).
5. V.M. Goldschmidt, F. Ulrich, T. Barth. “Skrifter Norske Vindenslaps-Akad” *Mat. Naturv. K1*. **Volume 5** (1925).
6. E.A. Aitken, S.F. Bartram, E.F. Juenke, “Crystal Chemistry of the Rhombohedral $MO_3.3R_2O_3$ Compounds” *Inorg. Chem*., **Volume 3**, pp. 949 (1964).
7. M. Amaya, K. Une, M. Hirai. "Heat Capacity Measurements of $U_{1-y}Gd_yO_2$ (y= 0–0.27) from 325 to 1,673 K." *Journal of nuclear science and technology*. **Volume 41 n2**, pp. 108-115 (2004).
8. M. Durazzo, H.G. Riella, IAEA Advanced Fuel Pellet Materials and Fuel Rod Design for Water Cooled Reactors (2009) 35.
9. L.R. dos Santos, M.Sc. Dissertation 1989, São Paulo University.
10. P. Scherrer, “Bestimmung der Grobe und her inneren Struktur von Loççoidteilchen mittels Röntgenstrahlen”. *Mathematish-Physikalische Klasse*, **Volume 198**, pp. 98-100 (1918).

11. J. I. Langford et all. “Profile analysis for microcrystalline properties by Fourier and other methods”. *Aust. Journal Physics*., **Volume 41**, pp. 173-187 (1988).
12. B. E. Warren, B. L. Averbach *“The effect of cold work distortion on XRD patterns” J. Appl. Phys*., **Volume 21**, pp. 595–599, 1950.
13. B. E. Warren, “X-ray diffraction methods,” *Journal Applied Physics*, **Volume 12**, no. 5, pp. 375–383 (1941).
14. Young, R.A. (Ed.), “The Rietveld Method, International Union of Crystallography” Oxford University Press, Great Britain, 1993.
15. Rietveld, H.M., “A profile refinement method for nuclear and magnetic structures.” *J. Appl. Crystallogr*., **Volume 2**, pp. 65–71 (1969).
16. B. K. Gan, P. Smith, et al. “Quantitative phase analysis of bauxites and their dissolution products”. *International Journal of Mineral Processing*, **Volume 123** (2013), pp. 64-72.
17. A. Baena, et al., “Lattice contraction and lattice deformation of UO2 and ThO2 doped with Gd2O3”. *Journal of Nuclear Materials*. **Volume 467**, pp. 135-143 (2015).
18. D. Balzar et al. “Size-strain line broadening analysis of the ceria round-robin sample”. *Journal of Applied Crystallography***. Volume 37**, pp. 911-924 (2004).
19. A. V. Fedotov et al. “Theoretical and experimental density of $(U,Gd)O_2$ and $(U,Er)O_2$” *Atomic energy***, Volume 113**, (2012).
20. T. B. Lindemer, A. L. Sutton, “Study of nontoichiometry of $<U_{1-z}Gd_zO_{2+x}>$” *J. Am. Ceram. Soc.*, **Volume 71**, pp. 553-561 (1988).